

Schematic design of a proposed SAS-based seismic isolation for LCGT

Riccardo DeSalvo Ryutaro Takahashi

JGW-T1000249



LCGT seismic attenuation system

The LCGT seismic attenuation scheme is shown in figure 0

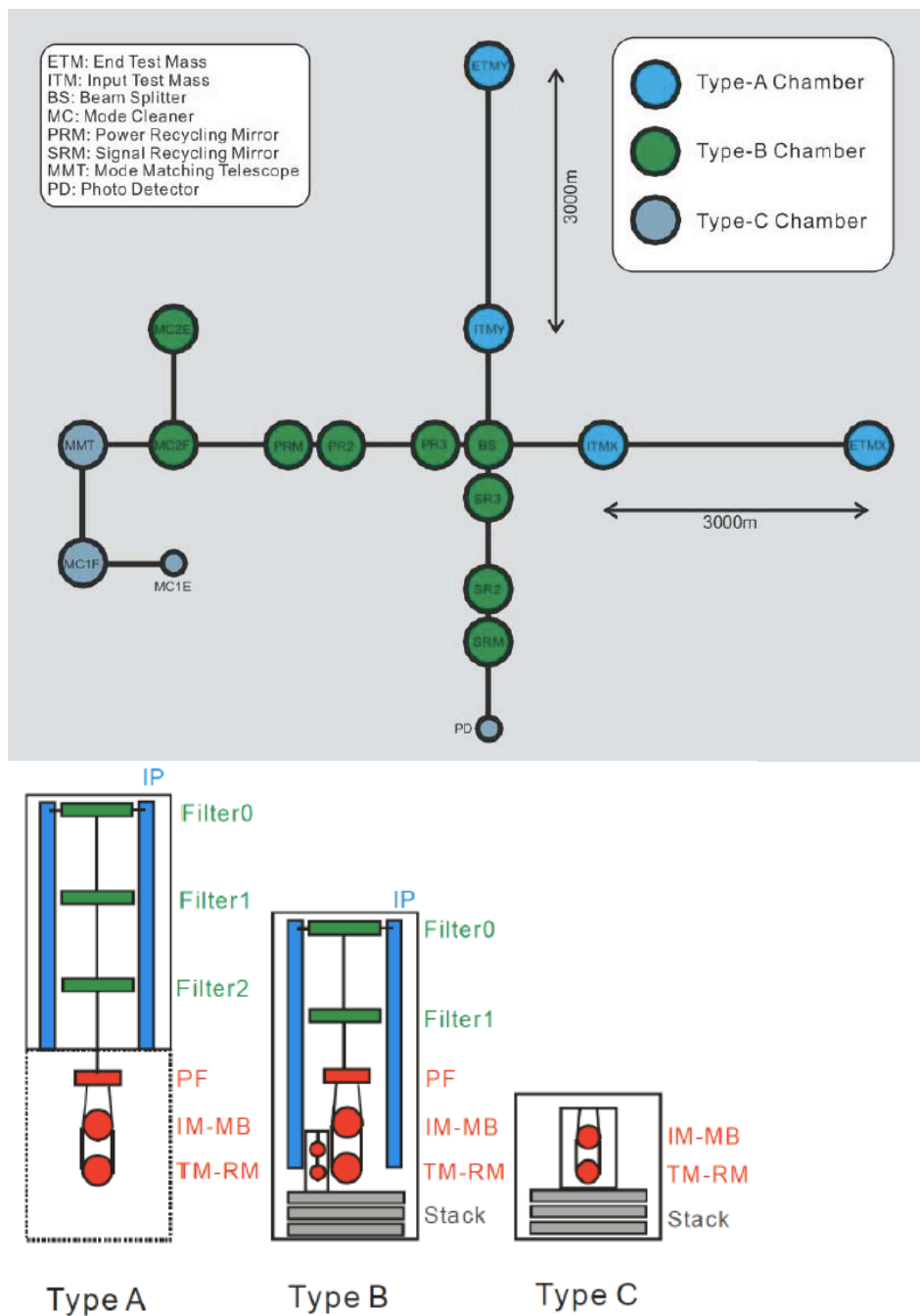


Figure 0: Seismic attenuation stations for LCGT. The test masses will be cryogenic, and require the highest level of seismic attenuation.

Schematics of the mechanics of the LCGT test mass seismic attenuation system

The design of the LCGT test mass seismic attenuation chain is based on three standard GAS filters, preceded by a pre-isolation and static-control stage. The pre-isolator stage is composed by a larger GAS filter mounted on short Inverted Pendulum legs.

The proposed pre-isolation stage sits directly on the floor of an utility tunnel to take advantage of the rock's stability. The attenuation chain resides below it, in a 900 mm diameter vertical pipe inside a 1000 mm borehole, which extends to the main LCGT tunnel.

The mirror suspension system and its cryostat reside in a separate chamber in the lower tunnel.

The minimal rock and reinforced concrete thickness between the two tunnels is 5 to 6 meter.

The aim of the seismic attenuation chain is to attenuate the seismic noise at or below the LCGT sensitivity level at the suspension point of the suspension payload. This requirement is necessary because it is expected that the thermal conduction requirements of the mirror suspension structure will allow for little attenuation in the horizontal direction and none in the vertical direction.

A 75 m long (15% slope) ramp is foreseen to access the upper from the lower tunnel.

The pre-attenuator sits in the upper tunnel, it is composed by a 50 cm tall inverted pendulum, essentially a copy of the successful HAM SAS IP [A. Stochino et al., *The Seismic Attenuation System (SAS) for the Advanced LIGO gravitational wave interferometric detectors*, Nucl. Instrum. Methods Phys. Res. **A 598**, 737–753 (2009)], supporting a 1.3 m diameter GAS filter, called Filter Zero. The mechanical resonances of the filter zero GAS filter and of the IP will be tuned substantially below the microseismic peak, at ~ 50 mHz. Some control will be necessary to reach that low resonant frequency [R. De Salvo, et al., *The Role of Self Organized Criticality in Elasticity of Metallic Springs; Observations of a new Dissipation Regime*, LIGO-P1000105, (2010)]

The pre-attenuator will be followed by three standard GAS filters tuned below 300 mHz. The filters will be equipped with magic wands to lower the attenuation saturation level and improve the performance from 60 dB to 80-90 dB per filter [A. Stochino et al., *Improvement of the seismic noise attenuation performance of the Monolithic Geometric Anti Spring filters for Gravitational Wave Interferometric Detectors*, Nucl. Instr. Meth. **A 580**, 1559–1564 (2007)] [Alessandro Bertolini, private comm. (2010)].

The large vertical separation between the pre-attenuator and the cryogenic payload allows for long suspension wires between the GAS filters, which in their turn yield lower pendulum resonant frequency (the 2.1 m long wires of figure 1 and a three-filter configuration gives 344 mHz pendulum resonant frequency per stage). These lower pendulum frequencies are necessary to match the GAS filter performance and produce uniformly increasing seismic attenuation in all degrees of freedom along the attenuation chain.

Larger separation between the tunnels would allow longer wires and lead to even lower resonant frequency, but the gain is rather slow. For example, a 10 m

vertical separation between the tunnels would give a 245 mHz pendulum resonance. This lower pendulum resonant frequency can be easily matched in the vertical direction with the GAS filter tuning. A proper simulation should be performed to simulate the overall chain attenuation power as function of tunnel separation and evaluate the real gain. Because longer wires are better, but the gain is slow above 5 m, we should decide the separation between tunnels based more on mining and rock stability considerations than on attenuation power ones.

The biggest concern about operating long attenuation chains is given by the yaw modes of the wire-filter torsional pendulum. Strong damping is necessary.

To produce the required damping without jeopardizing the attenuation performance, a heavy disk is suspended with three or six wires from filter zero, hovering just above filter 1. This filter is loaded with permanent magnets, whose field crosses an OHFC copper plate mounted on the roof of filter 1. The Eddy currents will damp all pendulum and torsion pendulum of the chain.

The introduction of magnetic damping will reduce the attenuation performance between filter zero and filter 1, but its ill effects on attenuation do not extend to the rest of the chain. Simulations will show if sufficient attenuation is available, or if a fourth filter will be necessary.

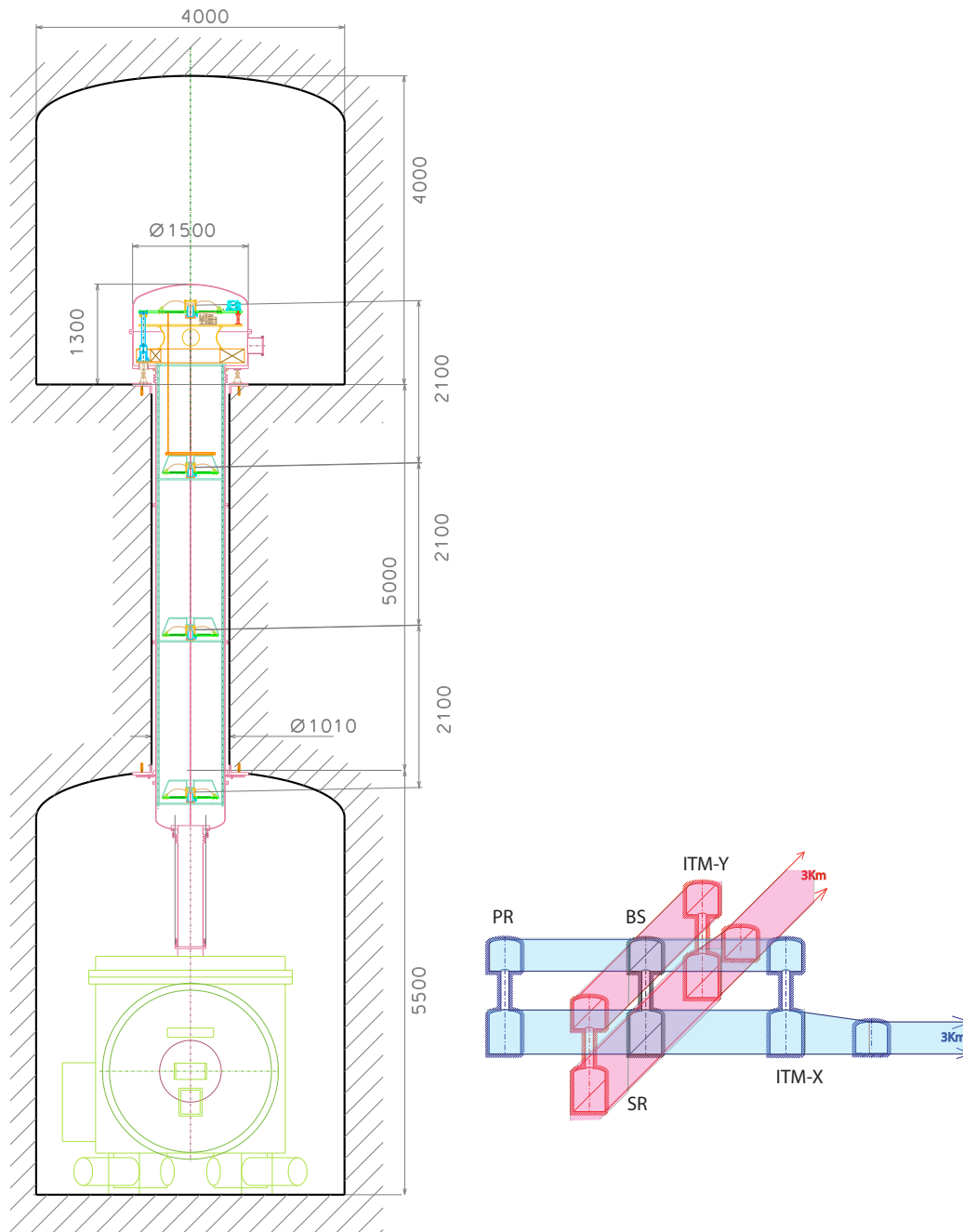


Figure 1: Schematic view of the LCGT test mass attenuation chain. The attenuation chain stretches between two separate tunnels. The pre-isolation stage sits on the floor of the top tunnel, the first and second filter hung inside the 900 mm down-pipe, while the third of the standard filters is suspended below the ceiling of the lower tunnel for easy access and loading of the cryogenic suspension payload. The filters are equally spaced for optimal damping from the top platform. Beam Splitter and Recycling mirrors may not require this attenuator scheme.

The design of the standard filter

The design of the standard vertical filter of the LCGT attenuation chains is now at version 5. Three standard filters, 730 mm in diameter, are foreseen. They will be numbered one to three starting from the top.

These three filters will be virtually identical, except for the number and width of the blades implemented inside each filter, which will be chosen to match the payload. Filter one will have all 12 blades, while filter two and filter three will have 10 and 8 blades respectively.

A larger filter, 120 mm diameter, called filter zero, is used at the top stage, to suspend the larger load, to provide attenuation at the lowest frequencies, and to facilitate the connection to the Inverted pendula and to the ground. This larger filter will be a scaled up version of the standard filter.

The function and the configuration of the standard filter is the same of the TAMA-SAS filters [R. Takahashi, et al., *Operational status of TAMA300 with the seismic attenuation system (SAS)*, Class. Quantum Grav. 25 114036 (8pp) (2008)] only with larger payload and lower working resonant frequencies.

The 12 GAS blades of the standard filter are virtually identical to those used in TAMA SAS, except for the number of blades and the attachment scheme at the two ends.

The new blade attachment scheme uses separate blades. The blades' tips join at a central keystone. The blade clamps at the outer diameter are mounted on radial slides to allow for easy frequency tuning.

This scheme was developed for and successfully tested on the HAM SAS prototype, and further tested by AEI SAS and NIKHEF SAS.

It allows easy match of any payload, by simply changing the number of blades per filter, as well as their thickness and width.

Up to ~500kg can be suspended from a fully loaded standard filter.



Figure 2: View of a standard filter loaded with 12 blades. The blades are flat at construction. They arch under load and wedge against a central keystone (blue) that support the filter's payload via a double-nail-head suspension wire. Each blade's base is held by a clamp with a 45° blade launching angle. Each clamp sits over the flat base plate of the filter, and can slide forward for frequency tuning. After tuning, the blade clamp is locked by two lip clamps. An end range ring (grey) above the keystone holds the blades under compression when the payload is removed. Six screws mounted on this ring, three pushing against the keystone, and three extending through it, delimit its oscillation range of $\sim \pm 2$ mm. Two wands, used to compensate the blade's center of mass effects, and two compensation blades are visible below the 12 suspension blades.

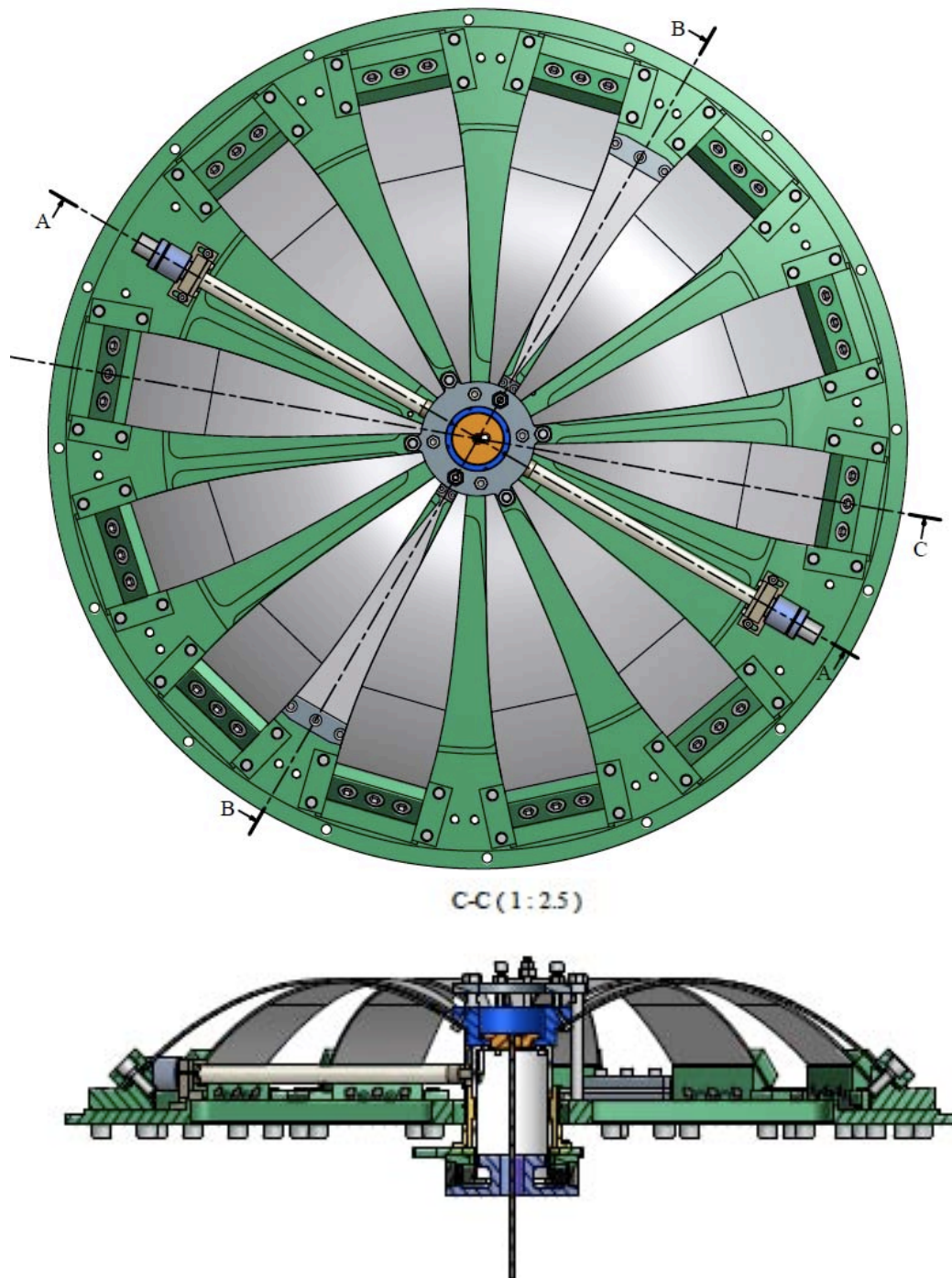


Figure 2: Top and side view of the standard filter. Note the two wands at 4:00 and 10:00 and the bimetal thermal compensation blades at 1:00 and 7:00.

Frequency tuning of the standard filter

To measure and tune its frequency the filter is loaded with a dummy mass. The dummy mass is adjusted until it floats between the end stops. The dummy mass is further adjusted until the vertical point of minimal frequency (maximal compression) is identified. This is the vertical working point of the filter. Its vertical resonant frequency is measured.

The vertical mechanical frequency tune of the filter is then obtained by changing the radial compression of the blades against the central keystone. More compression yields lower resonant frequency, excessive compression leads to bistability.

The radial compression changes are applied on pairs of opposed blades, to maintain symmetric load on the keystone. To change the radial compression a temporary tool (figure 3) is mounted around the lip clamps pushing against the blade clamp. The four screws of the lip clamps are loosened, the two radial screws on the tool are used to advance or retract the blade clamp. The locking screws are finally re-tightened and the tool is reused on a different blade.

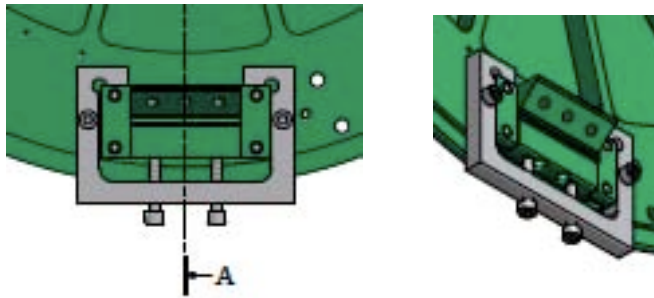


Figure 3: Tool designed to change the radial compression of the filter's blades.

Center of mass compensation of the standard filter

The vertical attenuation performance of the bare blades of the filter is limited to 60 dB by the Center Of Percussion (COP) effect. It can be compensated by adding a counterweighted wand in parallel to the suspension blades. The wand (Figure 4) is hinged on the GAS filter base plate, with the wand on one side, and a tuneable counterweight on the other side of the hinge.

The tip of the wand is hinged on the filter keystone.

Stochino demonstrated GAS filter attenuation up to 80 dB with aluminum wands, Bertolini improved it to 90 dB with more rigid Titanium Nitride wands [A. Bertolini, private communication, 2010].

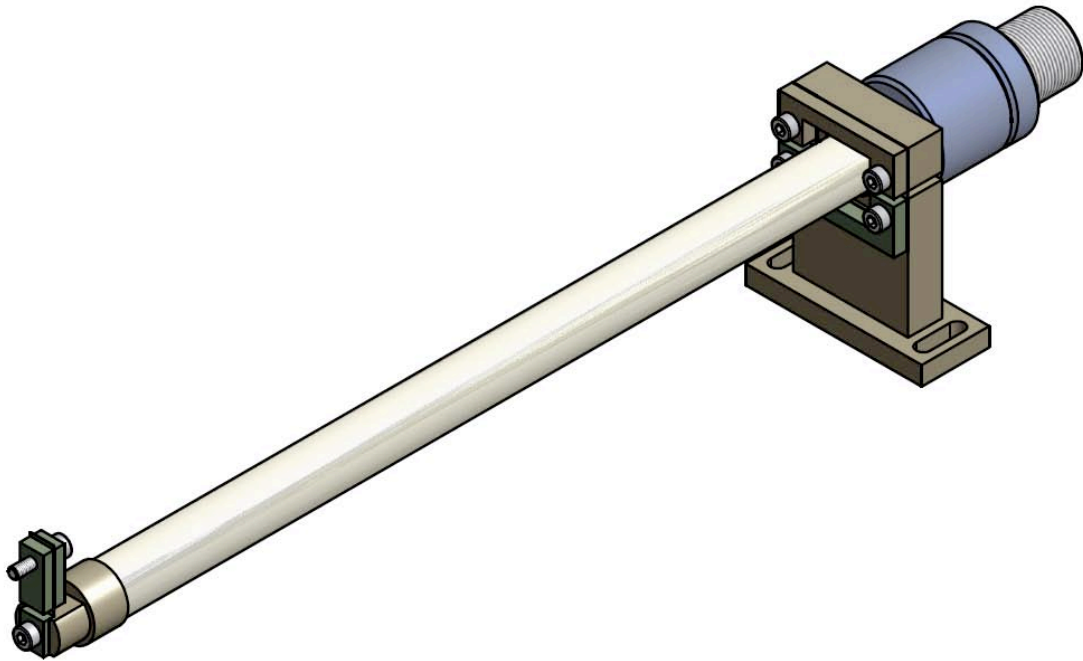


Figure 4: Magic wand used to compensate the blade's center of percussion effect that limits the filter attenuation performance. COP compensation can be tuned by adjusting the position of the two counterweights (blue) along a fine threaded back end.

Thermal compensation issues

The second stage of LCGT will feature cryogenic payloads. It is therefore likely that the LCGT filters will need to cope with the challenges of operation in the vicinity of a cryogenic environment.

Although the seismic attenuation chain itself is not cryogenic, it may be exposed to segments of solid angle at different and changing temperatures. This may lead temperature gradients inside the filter and changes of the filter's operating temperature.

This is a problem because the Young's modulus of the maraging blades changes by $2 \cdot 10^{-4}/^{\circ}\text{C}$. The filter payload lifting capabilities change by a corresponding amount, as much as $1 \text{ N}/^{\circ}\text{C}$ for a 12 blade filter. In addition temperature gradients may lead to a tilts of the keystone. Steps are necessary to mitigate both effects.

Thermal shielding of the standard filter

To avoid thermal gradients we enclosed the filter in a shell, which defines a local and uniform thermal bath for the blades (see Figure 5).

The shell has also an important mechanical function, the nose at its center provides a convenient hooking point for the wire that suspend the filter from the previous filter.

This hooking point, as well as the hooking point for the payload on the keystone, are located near the filter center of mass, to produce low frequency tilt frequencies.

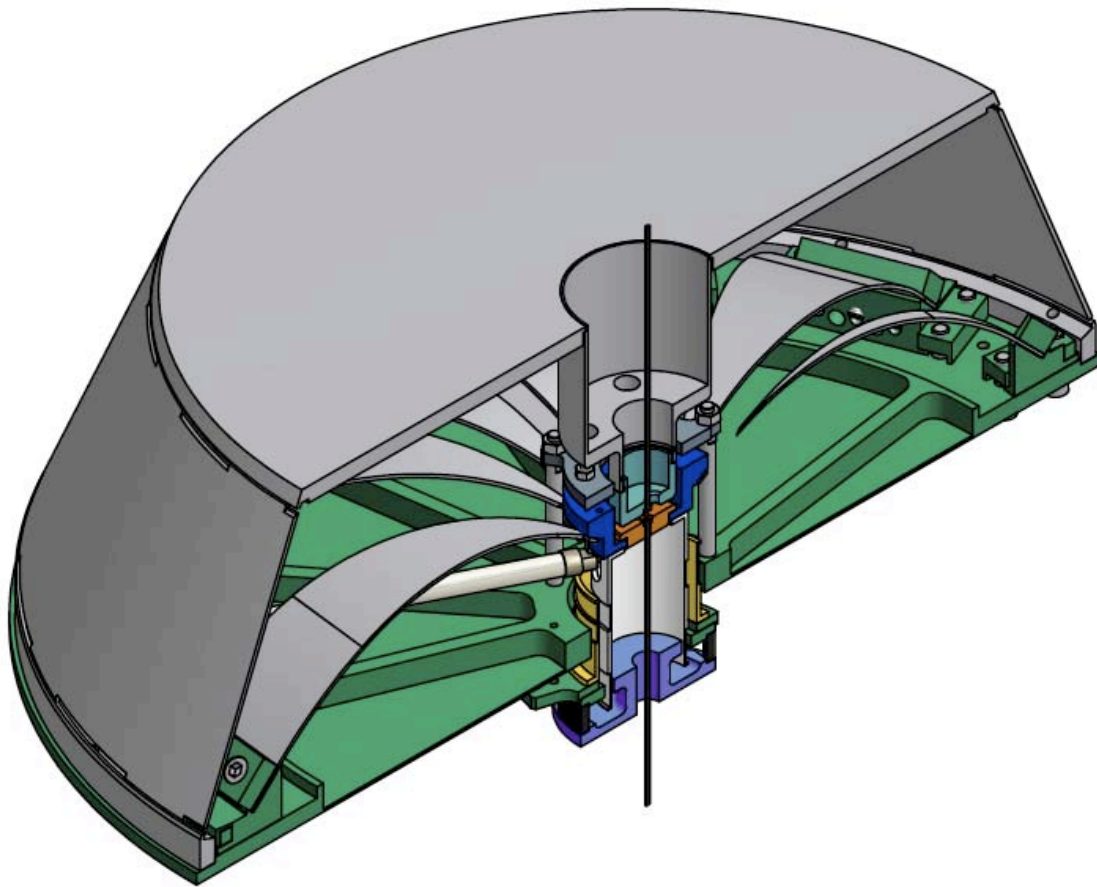


Figure 5: The standard filter is fully enclosed into a shell. The shell has two functions: thermal shield against asymmetric thermal loads, and hooking point for the wire that supports the filter.

Thermal compensation of the standard filter

LCGT is expected have transients from warm to cooled state, which, over long time scales, may change the working temperature of the standard filters by a few degrees. This problem will affect mostly the lowest filter, which will be closest to the cryostat.

To reduce the effects of these transients the filter body will be polished and possibly gold plated on the lower surface exposed to temperature changing colder bodies. A polished bottom will reduce the thermal conductivity towards the colder surfaces below, and slow down the filter thermal response to its transients. The aim is to cause all thermal variations to be slower than the thermalization time inside the shell.

The top surface would be left coarse and oxidized, with the largest possible black body coefficient, to establish preferential thermal equilibrium with the upper vacuum chamber, which is supposedly more thermally stable.

Because of the low frequency tune (soft spring) and of the relatively high thermal changes of Young's modulus in Maraging ($\sim 2 \cdot 10^{-4}/^{\circ}\text{C}$), any uncompensated change in temperature will generate a relatively large change of the filter's working point. Two techniques may be used to compensate, either in alternative or in parallel.

We are designing an internal thermal compensator based on a bimetal blade, mounted in parallel to the GAS blades. The bimetal blade is designed to provide a thermally changing force that will compensate the increase of Young's modulus at lower temperature. Like the magic wands, the bimetal blades will be fastened on the filter base plate at one end, and hinge on the keystone at the other end. The compensation bimetal blades will either mount below the filter main blades or replace a pair of GAS blades (this solution is not possible in filter 1, which is loaded with all 12 blades).

In alternative a small electrical heat radiator in slow feedback, illuminating the top of the filter, may be used to maintain a constant working temperature of the filter even in case of cold leaks. Filter one and filter zero, which are not exposed to changing thermal loads from the cryostat.

Wire hooking procedure of the standard filter

The filter's suspension wires are double nail head wires, machined from a solid rod of Maraging steel, longer but of the same type of the wires used in TAMA SAS. The split cup fastener type used in TAMA SAS is unsuitable for the function in LCGT. Both the keystone, and the shell nose are provided with receptacles snugly receiving the wire nail head and a side slot, similar to that that allows the insertion of the wire in bicycle brakes (see figure 6).

Three screws threaded in the range-limiting ring (grey) are used to push down on the keystone (blue), separate the keystone from the nose of the shell, and allow for wire insertion or extraction through the side hole.

These screws are reachable through holes in the filter's shell.

When unloaded the keystone is allowed to rest against the nose of the filter shell and both wires are imprisoned in place.

Both the keystone and the nose of the shell are provided with a replaceable central insert. The relative position between the filter suspension point and the filter center of mass can be changed by replacing these inserts. This relative position defines the filter tilt resonant frequency.

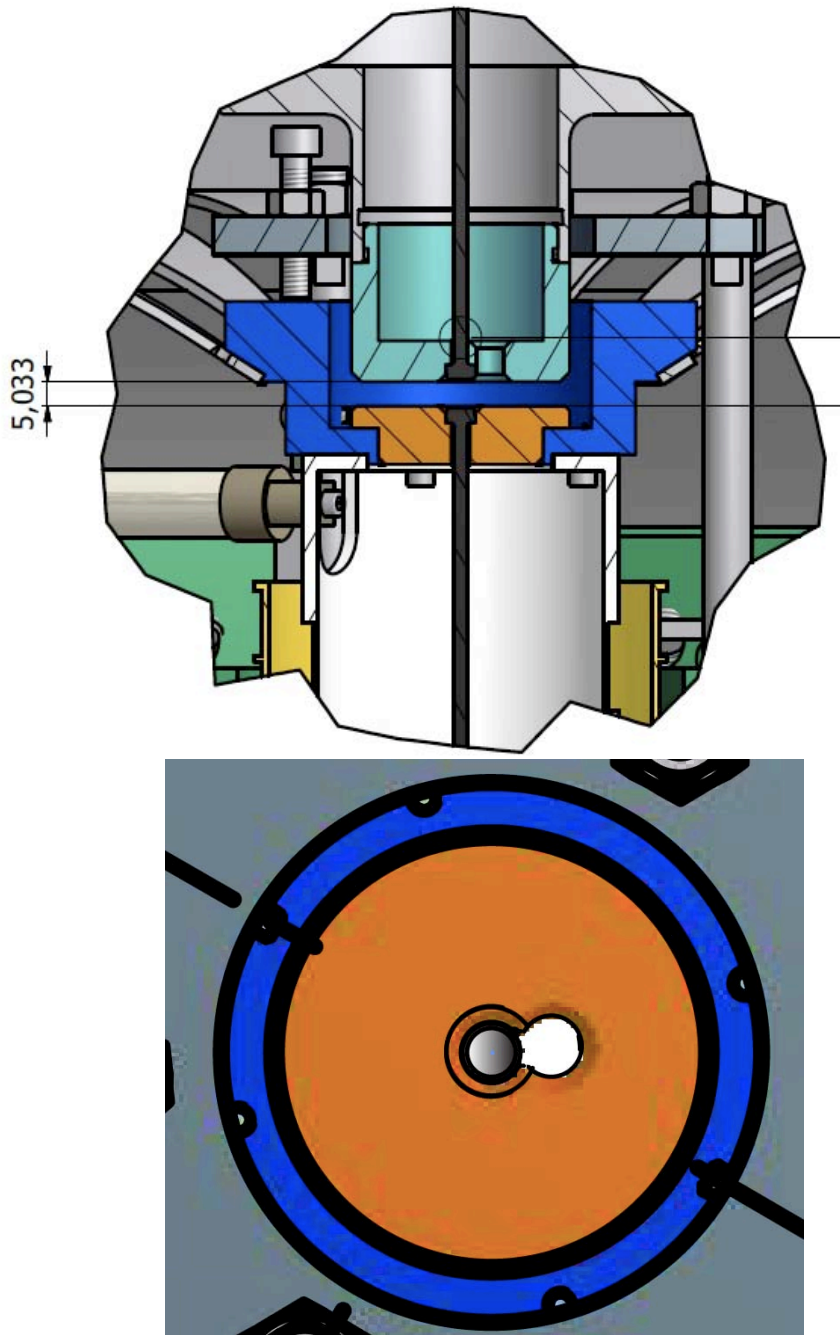


Figure 6: Details of the attachment of the wires to the filter. Side and Top view.

Load corrections of the standard filter

The load carried by the standard filter is fixed by the number, width and thickness of its blades. Most blades will be identical, lifting ~ 40 kg each. As blades always mount in pairs, eliminating a pair generates a load reduction of ~80 kg.

Smaller steps in payload can be achieved using pairs of narrower or thinner blades.

The standard filter needs to be loaded with its exact payload. After fixing the filter's nominal payload, the actual payload needs to be fine tuned to the filter's nominal payload to bring the filter to float at its working point. This fine-tuning is achieved by adding or removing some ballast mass from the next filter or from the suspension structure below.

This operation should be always performed starting from the lowest filter, and working the way up the chain. Attention must be paid to ambient temperature, as it can change the values of optimal load.

It is foreseen that each filter, weighting ~87 kg when fully loaded with 12 blades, will carry approximately 10% of ballast weight.

Filter 1 is obviously the most loaded, as it has to lift also the mass of filter 2 and filter 3, weighting ~90 kg each. A payload of up to 300 kg is foreseen, with no modifications.

Load reserve. The LCGT load requirements should be easily met by the proposed standard filter. However future evolution with possibly heavier mirrors may require even larger payloads. It is useful to evaluate how much more load can be imposed on the standard filters by changing blades and without requiring changes of the filter's physical shape.

Nominally the shape of the blades is such that the radius of curvature is kept as constant as possible along the blade, for optimal use of the material's strength. Simulations made at NIKHEF recently showed that the stress distribution is not constant and that a small modification of the blade's profile leads to a 10% reduction of the peak stress. This would allow the use of 10% thicker blades, which carry 33% more load, with no additional stress on the material.

Higher stress levels are also nominally possible [N. Virdone, et al., *Extended-time-scale creep measurement on Maraging cantilever blade springs*, Nucl. Instr. and Meth., **A 593** 597– 607 (2008)] [M. Beccaria et al., *The creep problem in the VIRGO suspensions: A possible solution using Maraging steel*, Nucl. Instr. and Meth., **A 404** 455– 469 (1998)], but not as thoroughly tested as the ones tested at TAMSAS, LIGO-SAS, AEI-SAS and NIKHEF-SAS.

Center of mass and Tilt correction of the standard filter

As already mentioned, the tilt resonant frequency is coarsely tuned by changing the relative position between the filter suspension point and the filter center of mass. A fine tune of the tilt resonant frequency and of the static tilt of the filter is achieved by re-positioning ballast mass. The ballast mass is necessary to adjust the load of each filter; it will be bolted either to the top or bottom plate of the standard filters. Moving some mass from the bottom to the top plate will decrease the tilt resonant frequency and vice versa.

The lateral distribution of the mass changes the static tilt of the filter and can be used to level it.

Assembly procedure of the standard filter

The standard filter is equipped with up to 12 pre-stressed blades mounted between the base plate and the keystone.

Specialized tools are necessary to properly and safely pre-stress the filter.

The first tool is the holder that keeps the keystone in place while the individual blades are installed, until the load is transferred to the keystone's retaining ring. The tool bolts to the bottom of the base plate and grabs the keystone from below as seen in figure 7.

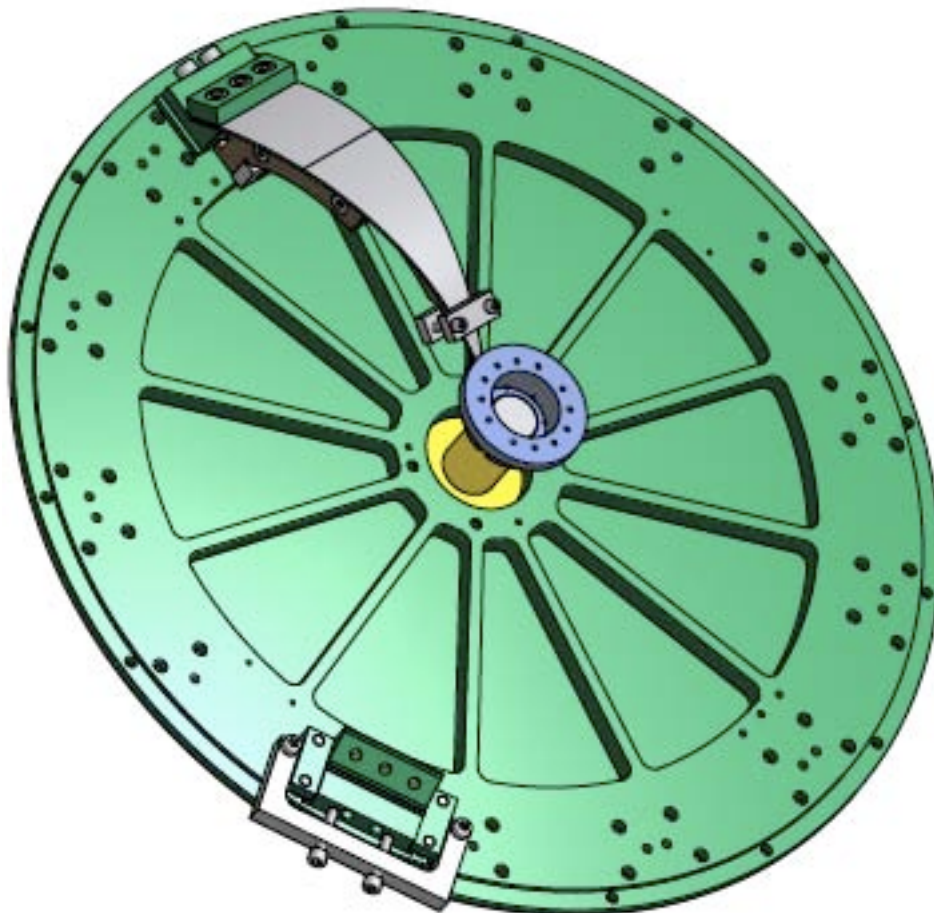


Figure 7: Keystone holder, shown in yellow at the center of the baseplate. Also shown at 11:00 a blade ready for assembly. Pairs of identical blades are always mounted in the same step, to insure symmetrical stress on the keystone.

Each blade needs to be pre-stressed individually, and kept under stress until the stress is transferred to the filter and keystone.
This is achieved with the tool illustrated in figure 8.

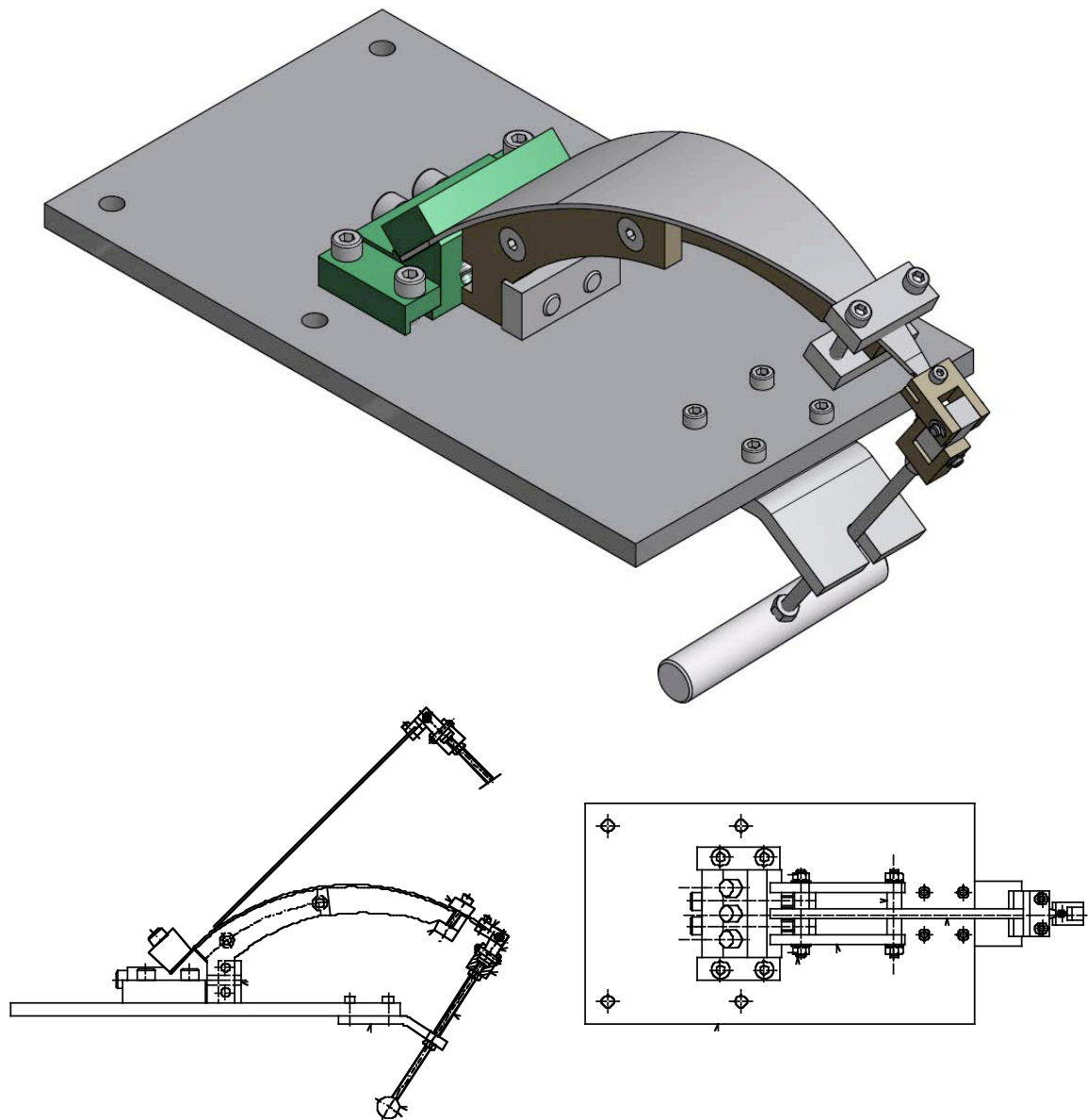


Figure 8: Pre-stressing procedure of each blade.
The blade (flat when unstressed) is mounted on its clamp (green), the clamp is locked on the stressing stand. The blade extends straight up with a 45 degree angle.
A properly shaped arched support (dark grey) is bolted to the blade clamp.
A pulling handle is attached to the tip of the blade.
The blade is stressed and rests on the arched support.
A tip clamp is used to fasten the blade's tip to its support
The pre-stressed blade assembly is released from the pulling handle and the stressing stand and it is ready for installation in a filter.

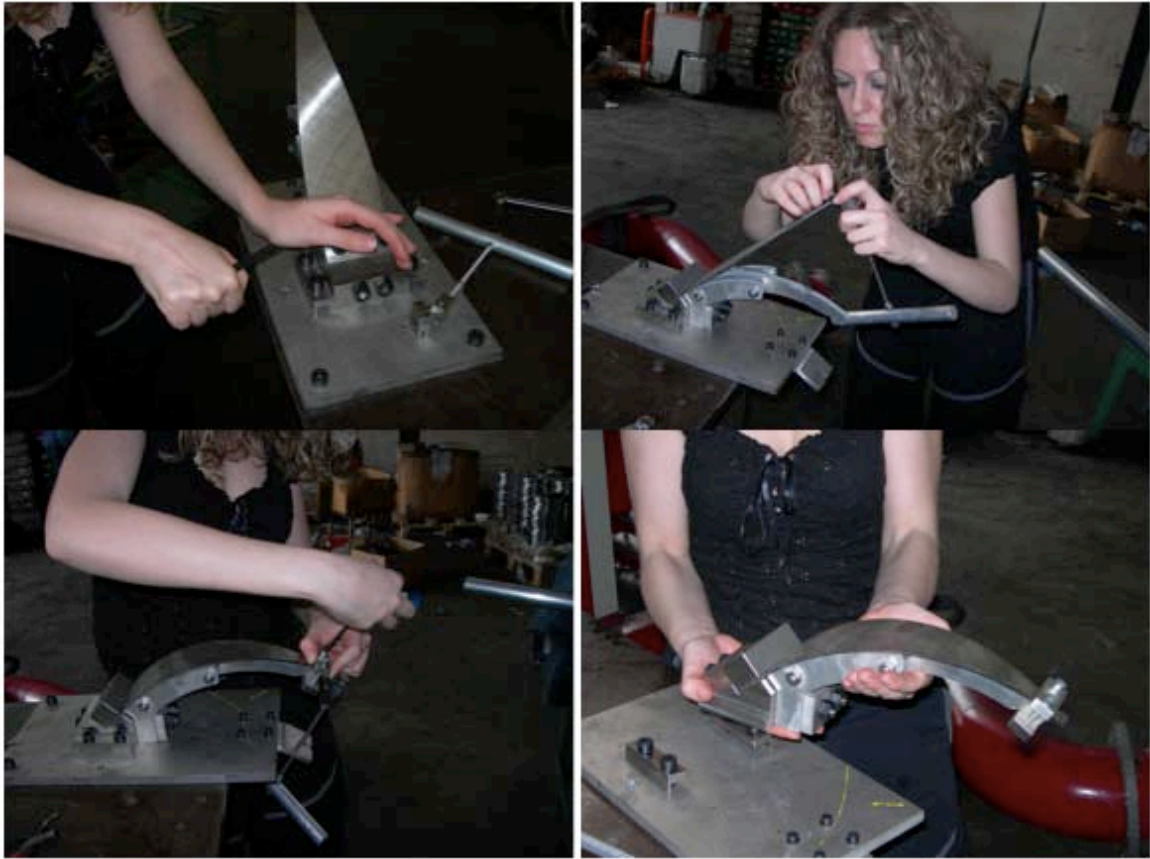


Figure 9: Blade pre-stressing sequence

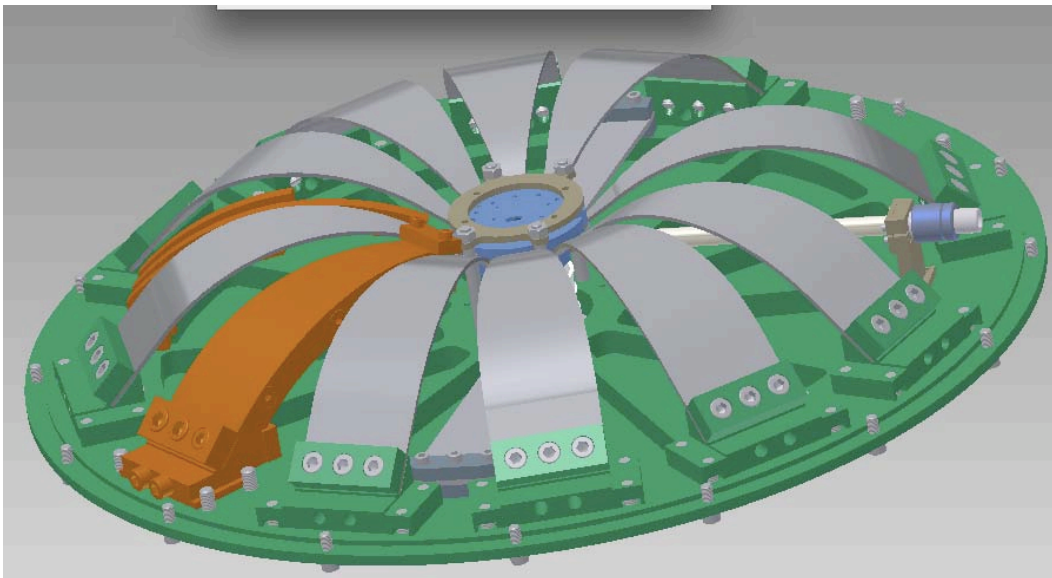


Figure10 : assembly of pre-stressed blades on a standard filter, and extraction of the blade holder (orange) from the angular space reserved from the magic wands.

Pairs of blades are mounted on the base plate, clamped down, and bolted to the keystone, then the support is freed up from the blade and extracted sideways as shown in figure 10.

There is no place to extract the blade's support between two adjacent blades. The support is extracted from the side before the next pair of blades is

assembled. It remains the problem of extracting the tool from under the last blade.

To allow extraction of the last blade, the 12 blades are spaced at less than 30 degrees intervals around the disk (see Figure 11) so that a wider angular space is left between blade 1 and 12 and between blade 6 and 7 to extract the last blade support. The space left is later used to implement the magic wands

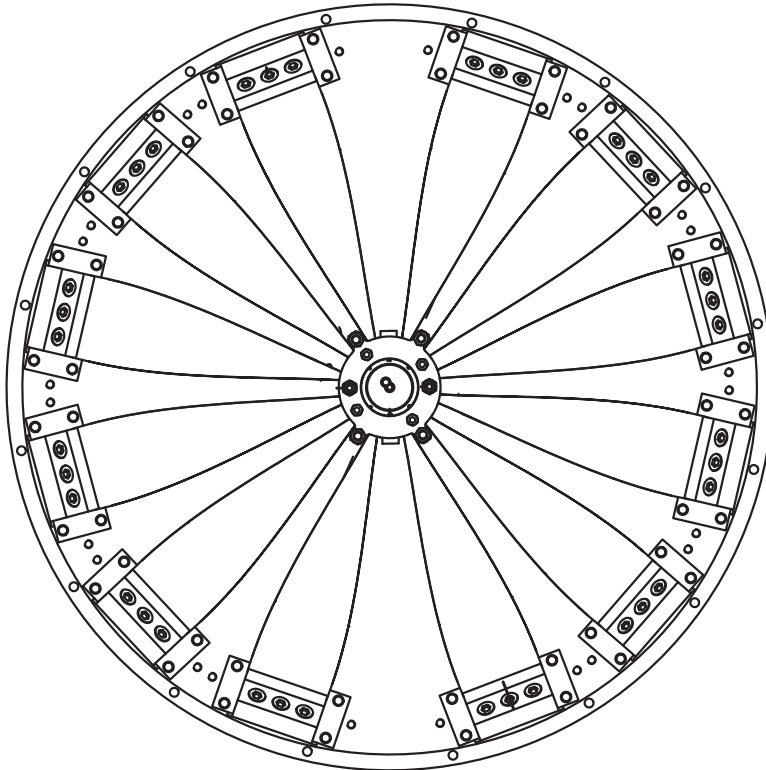


Figure 11: Illustration of the wider space left at 12:00 and 6:00 for the extraction of the blade's holder, and for implementation of the magic wands.

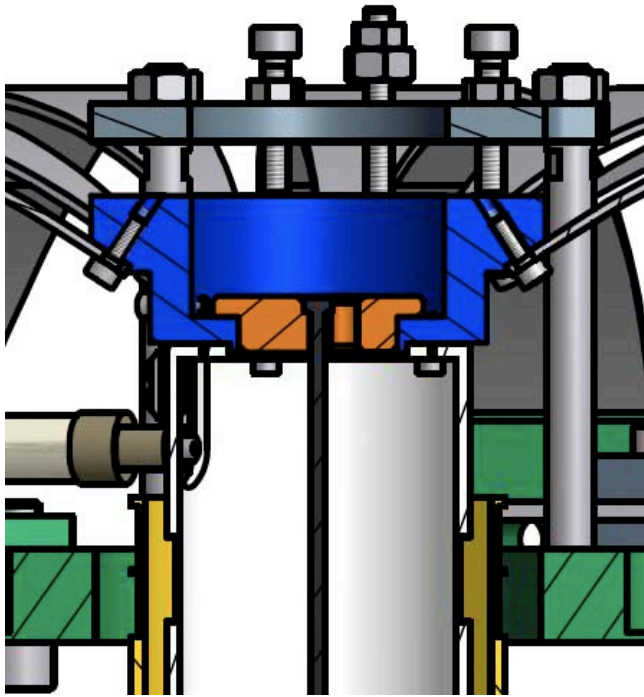


Figure 12: Stress transfer sequence from the keystone holder to the range limiter. The keystone range limiter (Dark Grey) is bolted to the base plate, above the keystone (Blue) and the stress is transferred to the range limiter by tightening the three pushing screws, then the keystone holder is removed from below the filter base plate.

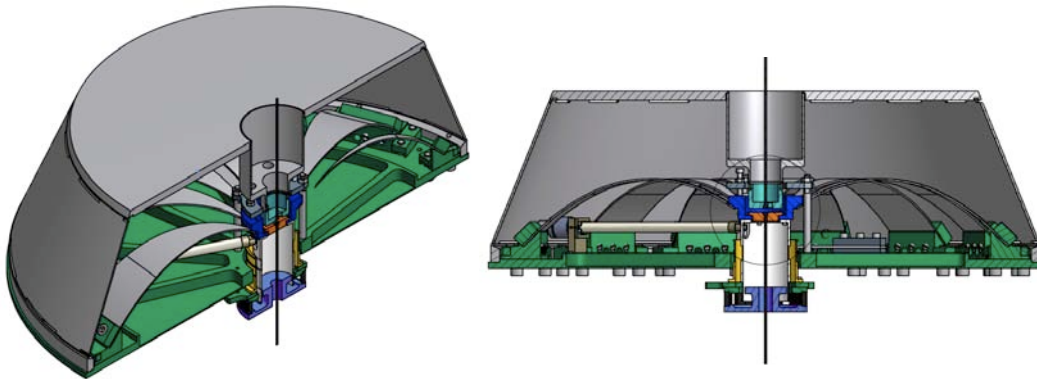


Figure 13: The external Shell is bolted to the baseplate when the filter is complete.

Assembly procedure of the attenuation chain in the borehole.

The test masses of the interferometer are the most sensitive to seismic disturbances. The proposed installation of the LCGT seismic attenuation chains for the test masses requires two superimposed tunnels. The bottom tunnel is the LCGT beam tunnel, the top tunnel houses the base of the seismic attenuation chains.

This is done to give the best mechanical stability to the seismic attenuation chains, taking full advantage of the underground location.

This configuration is recommended for the beam splitter as well.

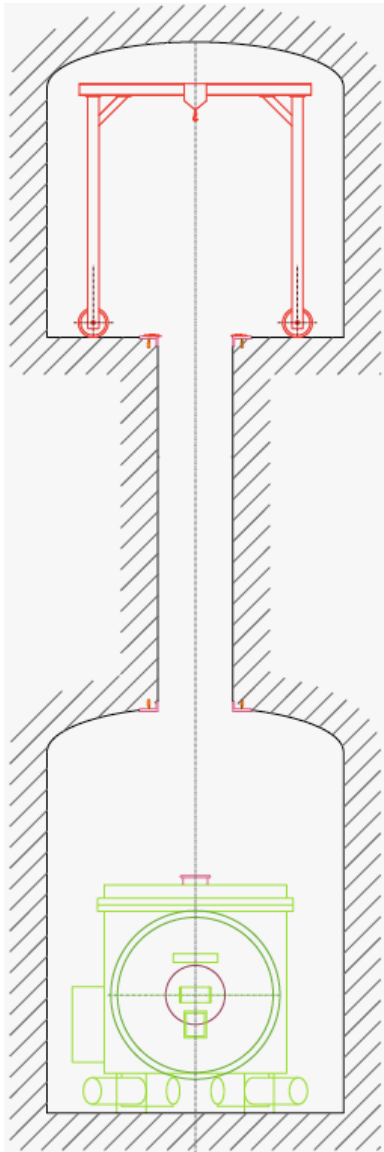


Figure 14: View of the overlapping tunnels. A minimal separation of 5 m between the tunnel (>1 tunnel diameter) is required for rock stability. Larger separation between the tunnels is equally good for the SAS, as longer wires produce attenuation at lower frequency. All implementation of the seismic system and of its vacuum system will be lowered from the top tunnel with the help of an A-frame crane.

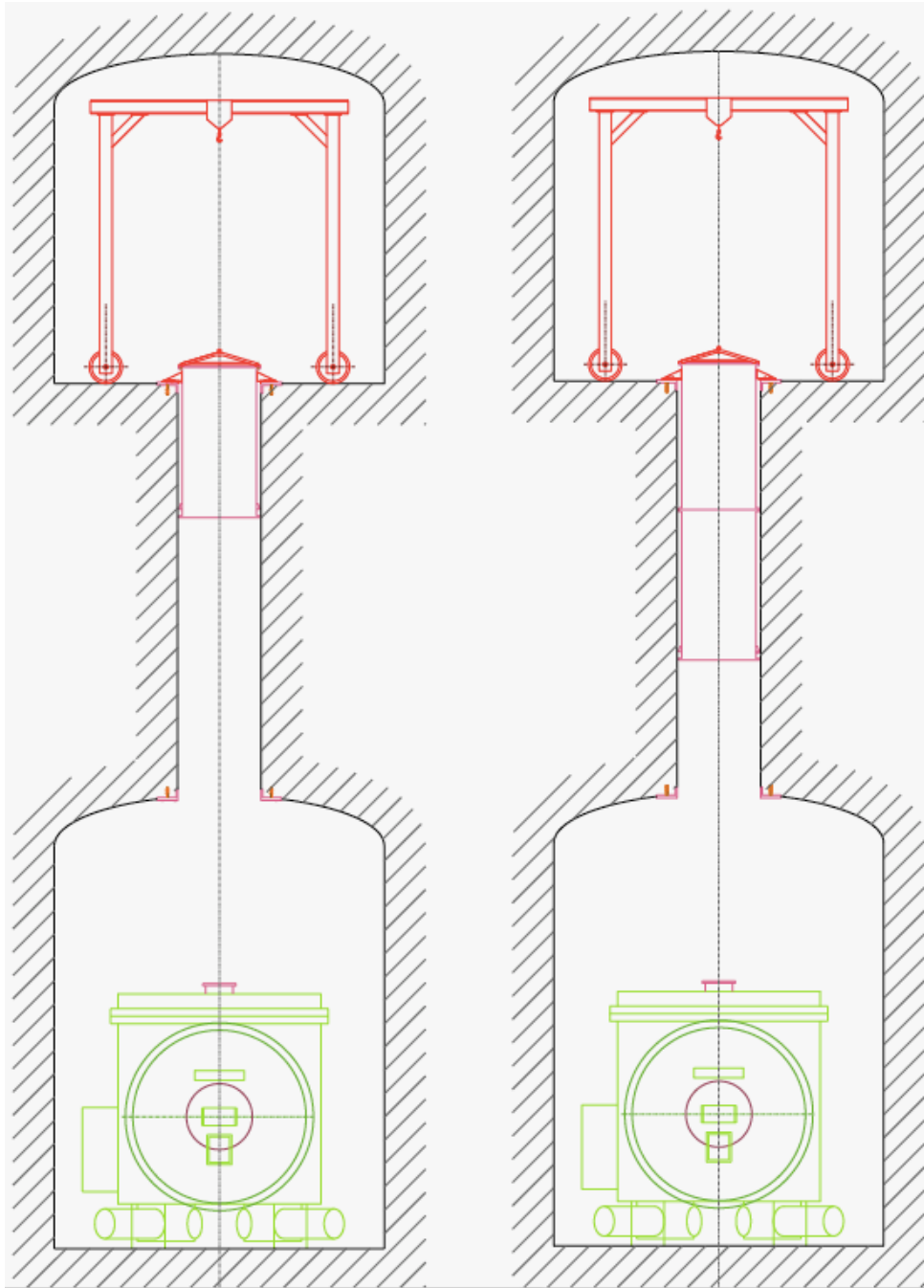
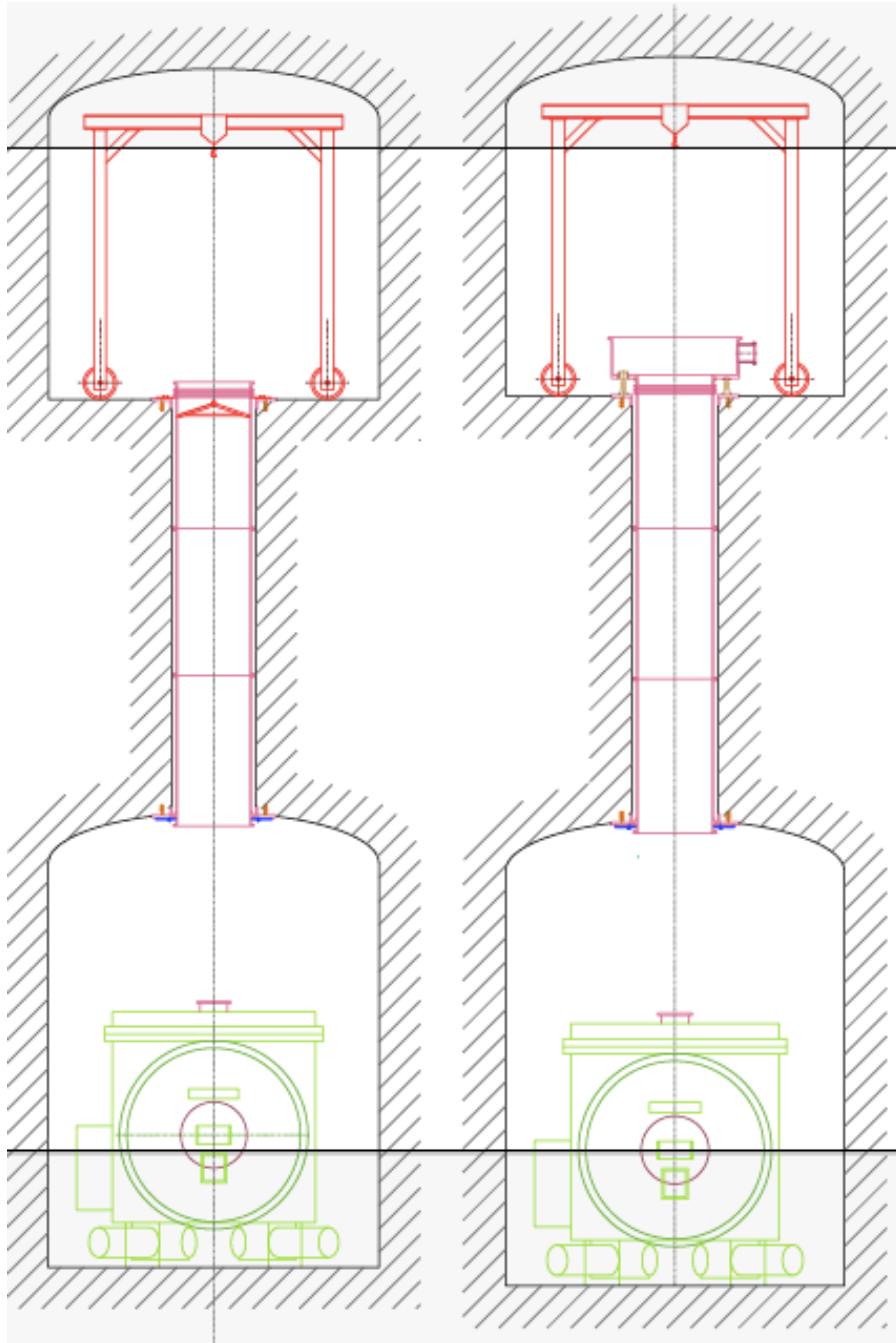


Figure 15: Sequence of installation of the vertical vacuum pipe down the 1000 mm diameter borehole

Panel 1, the lowest, pipe section is lowered with the crane partially into the borehole, and grabbed with a temporary clamping, to allow bolting of the middle section.

Panel 2, the lowest and middle pipe sections are lowered and re-grabbed, to allow mounting of the top pipe. After lowering a section, it has to be grabbed near the floor, to allow the bolting of the next section



Panel 3, the three pipes are lowered in place, a clamping ring is attached to the bottom pipe and bolted to the ceiling to hold the weight of the three pipes.
Panel 4, the bottom of the inverted pendulum vacuum chamber is bolted on top of the top pipe section

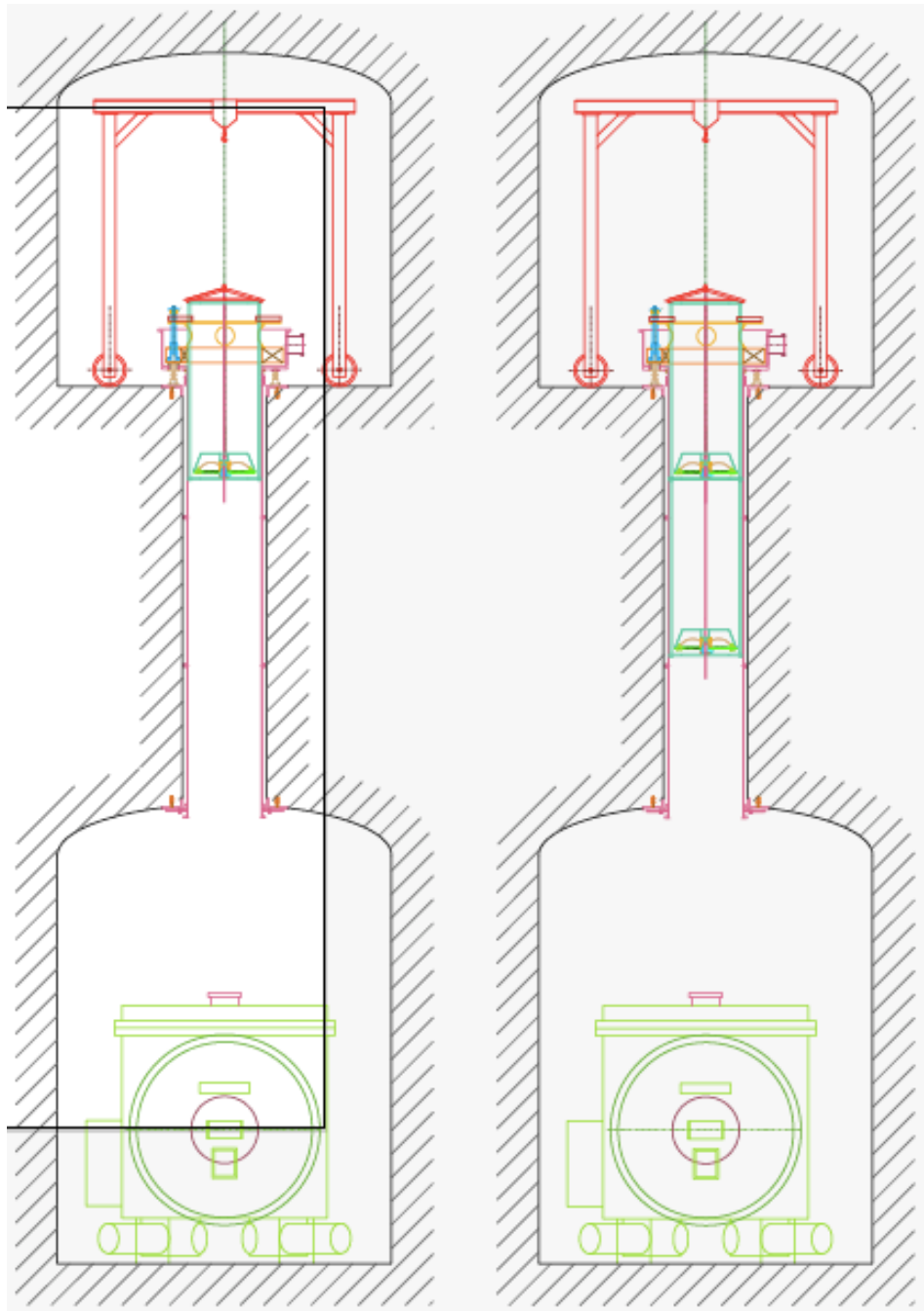
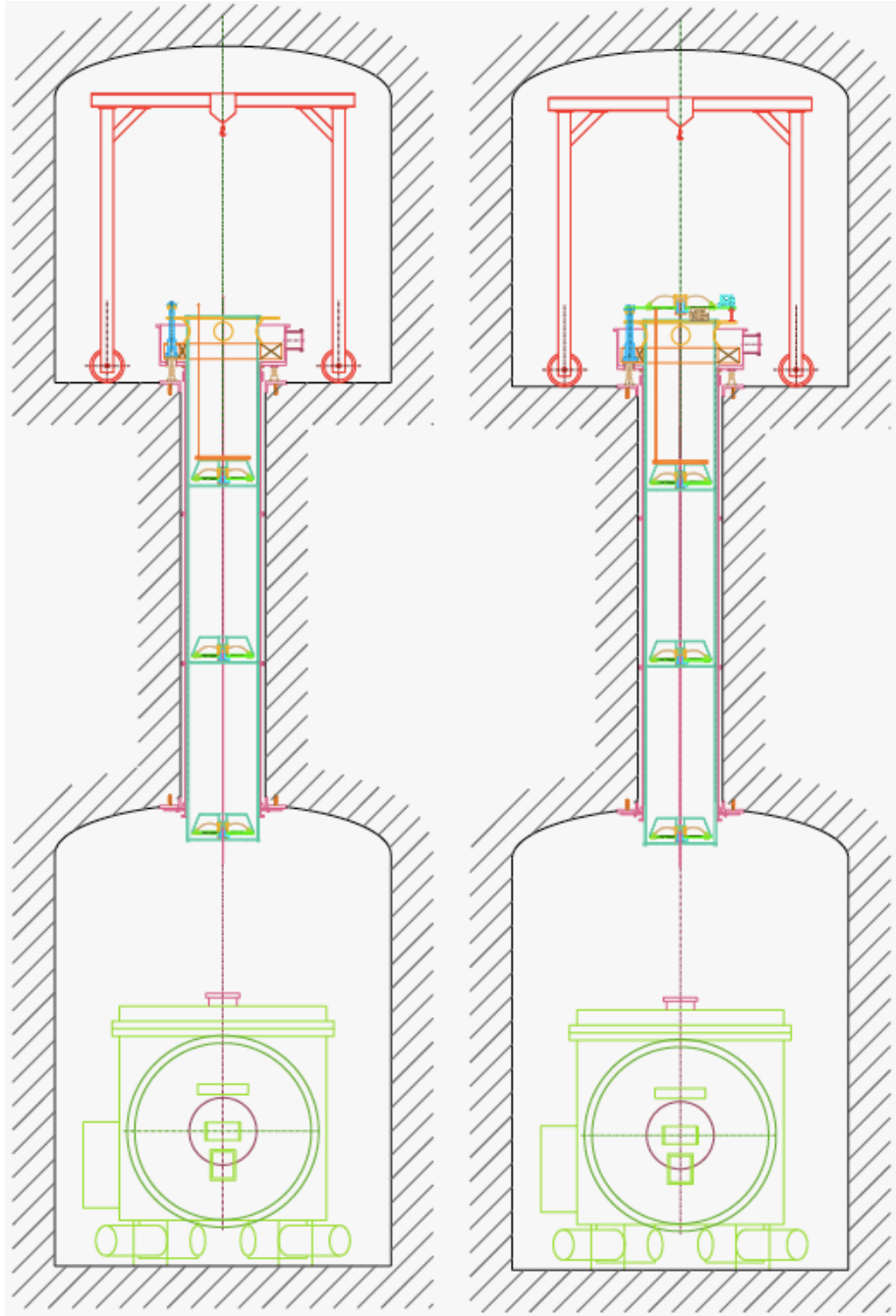


Figure 16: Sequence of insertion of the SAS chain.

Panel 1, the bottom filter is loaded with a dummy load, suspended from its wire from the crane, and tested for correct functioning. A safety structure (red) surrounds the filter, the safety structure is simply a steel ring supported by three rods. All cabling is prepared. The safety structure rods are grabbed. The filter is lowered on its safety structure. The safety structure is attached to the crane, lowered and re-grabbed.

Panel 2, a second safety structure is bolted on top of the first, the mid filter is attached to the wire of the bottom filter, the mid filter is hanging from its wire, and it is tested and cabled. Then both filters are lowered on their safety structure.

The safety structures are attached to the crane, lowered and re-grabbed.



Panel 3, the operation is repeated for the top filter

Panel 4, the filter zero, and the IP are attached to the top filter wire.

The safety structure is attached to the IP basement, the entire chain is lowered on its basement.

Now the bottom filter sticks out in the lower tunnel (in the topmost part of the cryostat) where it can be accessed from the side. Its dummy payload can be replaced with the real payload.

The problem for accessing the bottom filter, and then closing the vacuum to the cryostat chimney is unusual. It can be solved with a pot with an inverted flange, as schematized in figure 17.

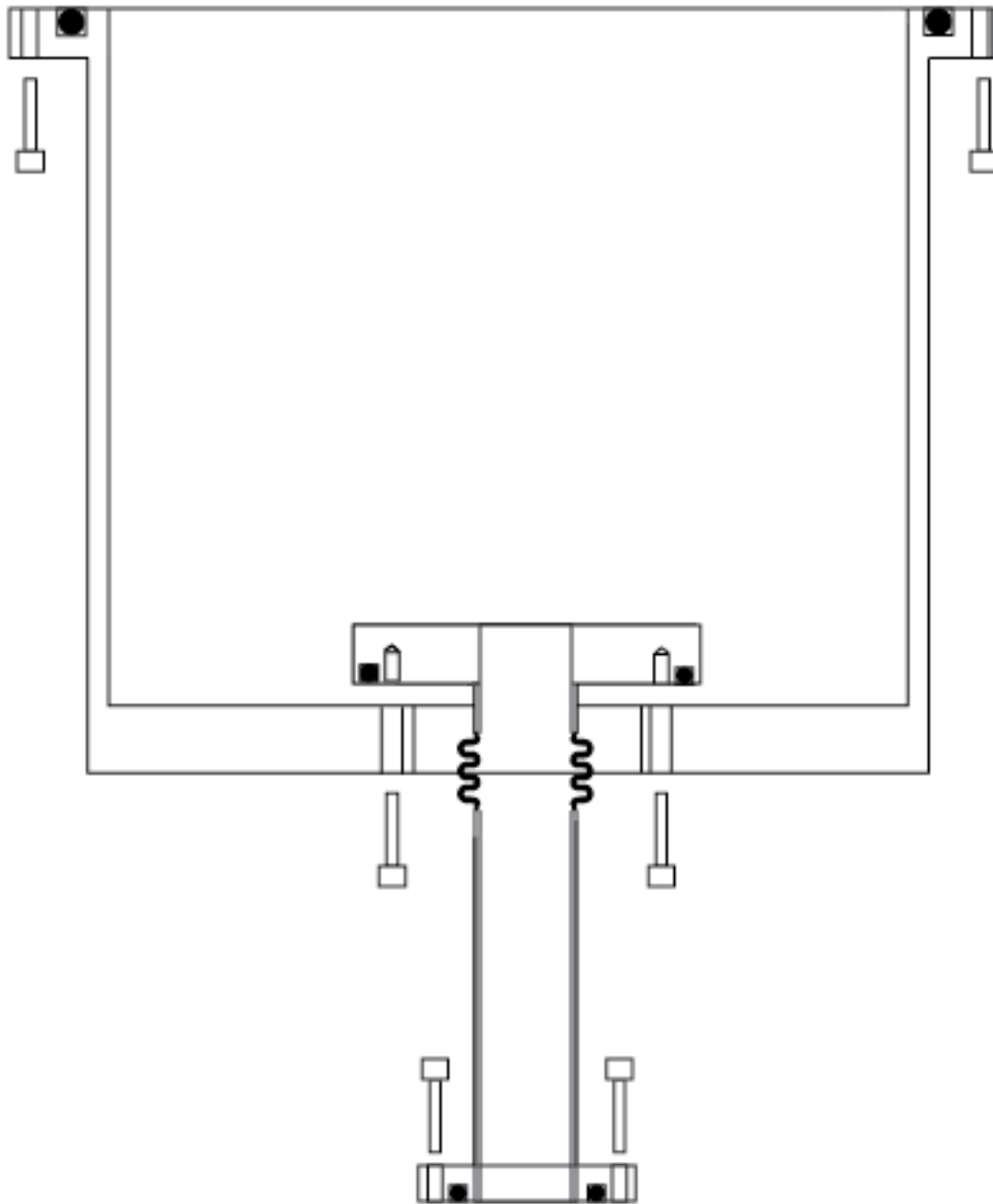


Figure 17: Scheme of the pot closing the vacuum from the 9000 mm pipes down the borehole to the cryostat chimney. The pot can slide along the cryostat's chimney. The Cryostat chimney has an inverted flange at the top, and a normal one at the bottom. It is first inserted through the bottom hole of the pot. The chimney is then sealed to the cryostat. Lifting the pot it is possible to bolt and seal it both to the 9000 mm pipe protruding from the borehole, and to the inverted flange of the chimney.

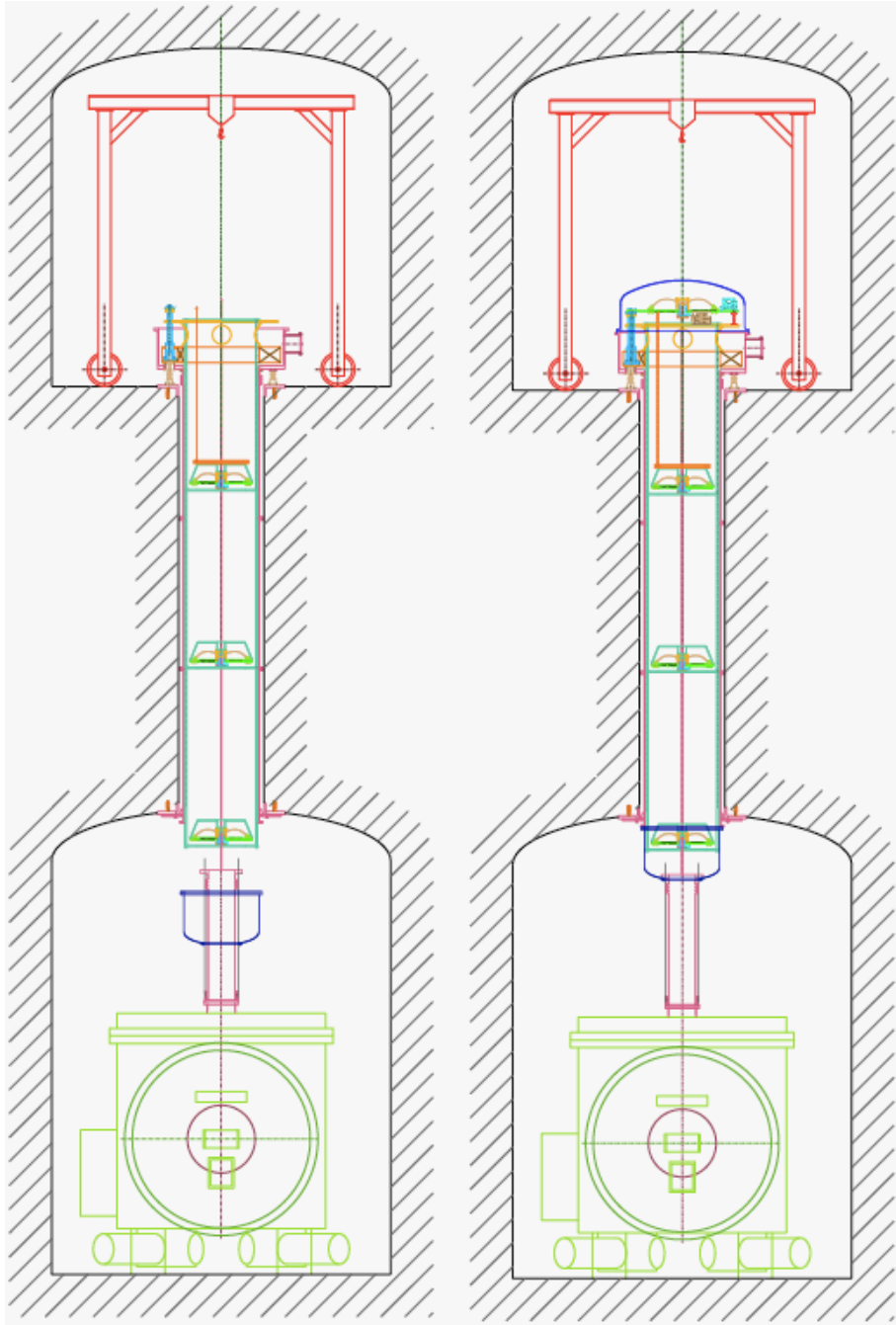


Figure 18: First panel, illustration of the access to the bottom filter. Second panel, sealing the vacuum sliding up the pot above the cryostat.

Schematics of the mechanics of the LCGT secondary mirror seismic attenuation system

The seismic attenuation for secondary mirrors is less demanding. The scheme proposed initially, figure 19 [Takahashi, f2f 100927], was essentially a copy of TAMA-SAS with the Inverted pendulum mounted on stilts.

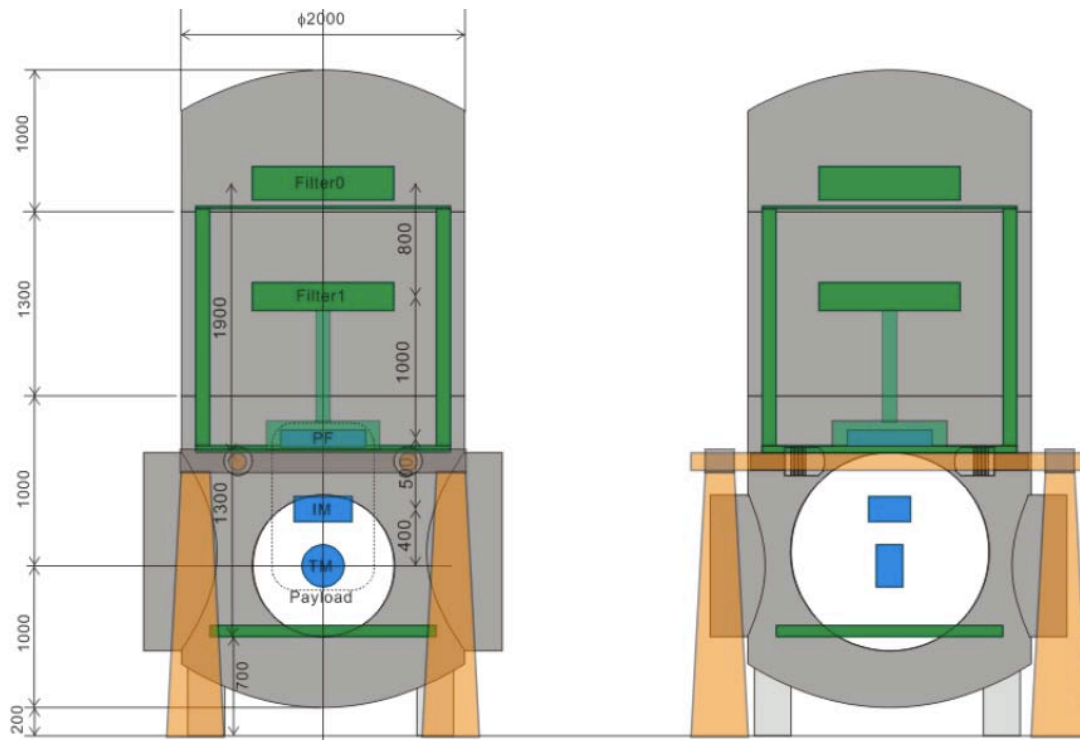


Figure 19: Schematic setup for the suspension of the secondary mirrors (Type B SAS)

The main problem with this scheme is that the stilts are flimsy and this configuration has been proven to enhance seismic noise.

The solution proposed to mitigate the stilts problem is to build a very rigid L-beam and sheet metal castle around the vacuum chamber, to support the pre-isolator as shown in figure 20.

It is relevant to remind here that the floor rigidity is very important.

It is useless to make rigid steel structures if the floor is not sufficiently hard.

When lining the tunnel and building the floor of the hall no loose refill should be allowed below the reinforced concrete floor. Solid concrete should be cast directly above native and un-fractured rock. Any loose rock or boulder should be removed before making the floor. Some anchoring of the floor, with short drilling and steel stubs connected to the reinforcement steel and to the steel footing of the castle.

The same IP, and GAS filters developed for the test mass suspension would be used for the pre-isolator and the attenuation chain of type B seismic attenuation. Modular structures will save time and money and will ease controls.

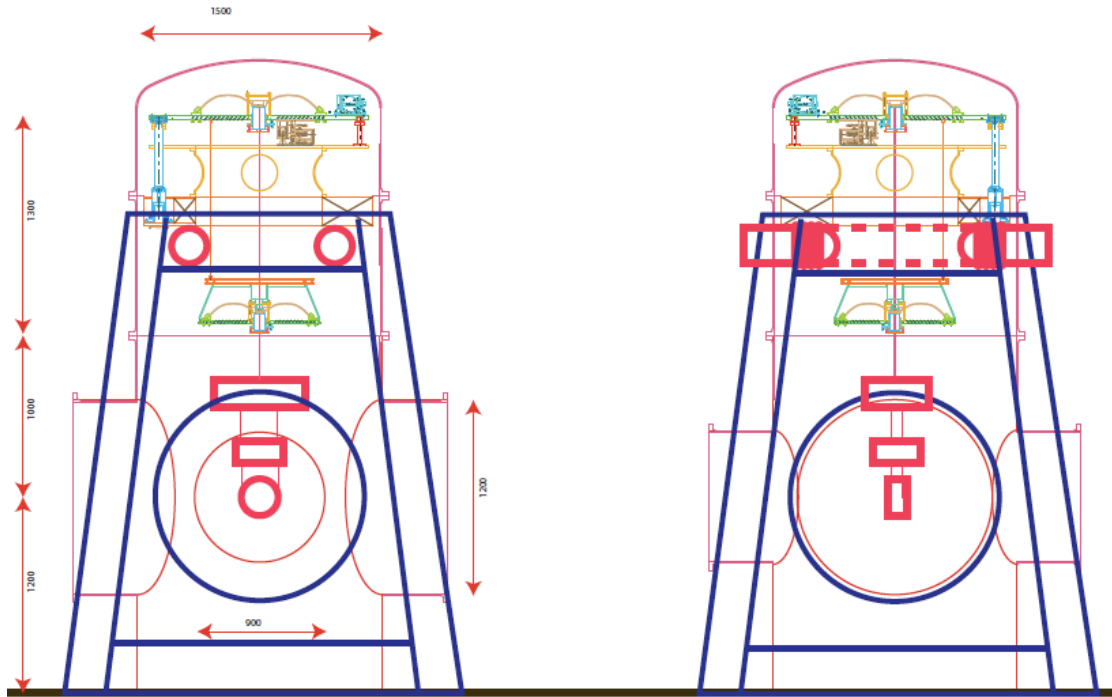


Figure 20: Schematic view of the mirror suspension for the secondary optics. The pre-isolator, at the top of the attenuation chain, is supported by a rigid external castle.

As in the case of the test mass suspensions, the vacuum tank has been reduced to 1.5 m diameter.

In type B and type C vacuum chambers (figure 19 and 21) optical benches 500 mm below the beam line are foreseen to support ancillary optics. Stacks or SAS seismic isolators are necessary.

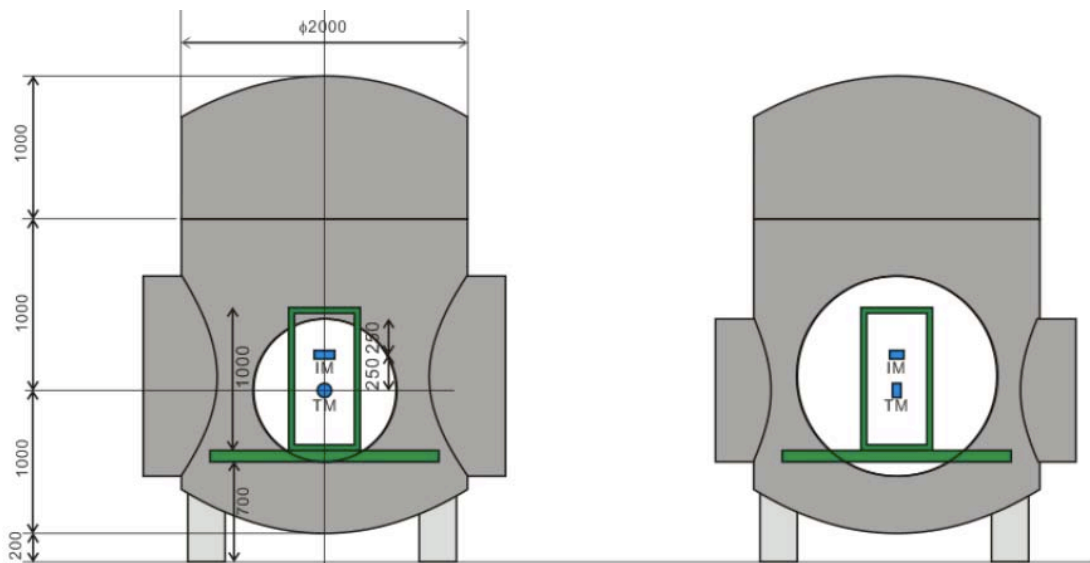


Figure 21: Schematic setup for the suspension of the auxiliary mirrors (Type C SAS)

There is little space between the nominal floor and the optical bench, for either SAS or stacks. A dugout under the vacuum chambers would be required to house the stack or the SAS table (figure 22). Because dugouts are difficult to make and inconvenient to work in, we suggest that the entire floor in the experimental halls be lowered by ~ 40 cm with respect to the floor in the tunnels, as illustrated in figure 23.

Note that the 2.5 x 2.5 m footprint of the castle allows vacuum chambers as close as 3 m center to center, as originally foreseen. A minimum separation between vacuum chambers of at least 4 m center to center is recommended

For the seismic attenuation of the auxiliary benches, we propose here a simplified version of HAM SAS, without accelerometers for inertial damping, and higher frequency tuning. LVDT and voice coil actuators would be retained for viscous damping and for positioning, but maybe no remote control stepper motor positioning.

Identical stacks or HAM-SAS systems would be used at the bottom of type B or type C chambers.

The vacuum chamber has been reduced from the initially proposed 2 m diameter to 1.5 m, the rationale is that an optical table larger than the 1.4 m diameter table foreseen here is of limited use with the 800 or 1000 mm vacuum pipes.

The savings in going from 2 m to 1.5 m diameter vacuum chambers is almost a factor of two.

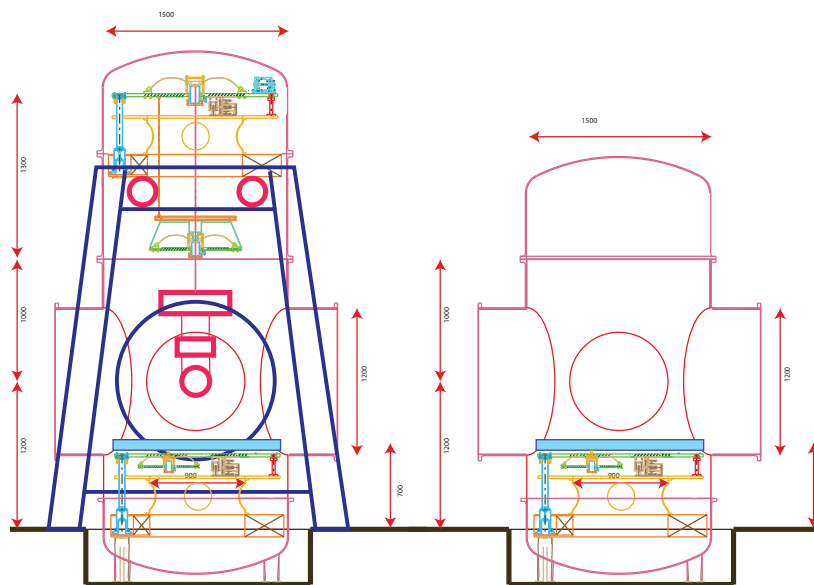


Figure 22: Illustration of HAM-SAS-like seismic attenuated optical benches in type A and type B vacuum chambers. Dugouts will be necessary below the vacuum chamber to house both the stacks and the SAS isolators.

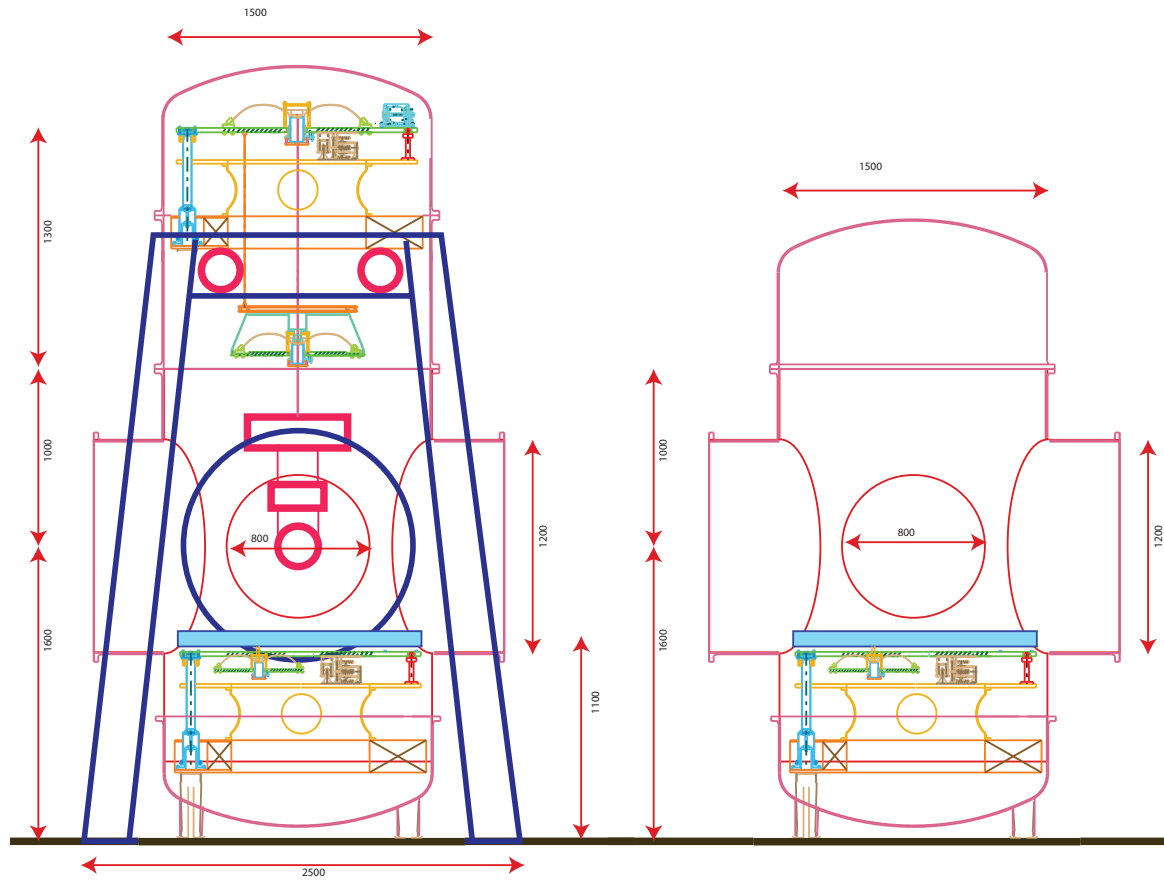


Figure 23: Illustration of the same HAM-SAS-like seismic attenuated optical benches. The dugouts have been eliminated in this illustration by lowering the floor of the hall by 40 cm.